Existence and topological stability of Fermi points in multilayered graphene

J. L. Mañes,[1] F. Guinea,[2] and María A. H. Vozmediano[3]
[1]*Departamento de Física de la Materia Condensada, Universidad del País Vasco, Apartado 644, E-48080 Bilbao, Spain*
[2]*Unidad Asociada CSIC-UC3M, Instituto de Ciencia de Materiales de Madrid, CSIC, Cantoblanco, E-28049 Madrid, Spain*
[3]*Unidad Asociada CSIC-UC3M, Universidad Carlos III de Madrid, E-28911 Leganés, Madrid, Spain*
(Received 19 February 2007; published 20 April 2007)

We study the existence and topological stability of Fermi points in a graphene layer and stacks with many layers. We show that the discrete symmetries (space-time inversion) stabilize the Fermi points in monolayer, bilayer, and multilayer graphenes with orthorhombic stacking. The bands near $k=0$ and $\epsilon=0$ in multilayers with the Bernal stacking depend on the parity of the number of layers, and Fermi points are unstable when the number of layers is odd. The low-energy changes in the electronic structure induced by commensurate perturbations which mix the two Dirac points are also investigated.

DOI: 10.1103/PhysRevB.75.155424 PACS number(s): 71.10.Ay, 75.10.Jm, 75.10.Lp, 75.30.Ds

I. INTRODUCTION

The recent synthesis of monolayer graphite[1,2] (graphene), the experimental ability to manipulate few layer samples,[3–5] and the observations of quasi-two-dimensional behavior in graphite[6] have awaken an enormous interest in these systems. The conduction band of graphene is well described by a tight-binding model which includes the π orbitals, which are perpendicular to the plane at each C atom.[7,8] This model describes a semimetal, with zero density of states at the Fermi energy and where the Fermi surface is reduced to two inequivalent K points located at the corners of the hexagonal Brillouin zone. The low-energy excitations with momenta in the vicinity of any of the Fermi points have a linear dispersion and can be described by a continuum model which reduces to the Dirac equation in two dimensions,[9,10] which has been tested by recent experiments.[4,5,11] Fermi points have also been found in the modeling of the low-energy band structure of multilayer systems both theoretically[12,13] and experimentally.[14,15] A crucial issue for both theory and technology is the possibility of controlling the opening of a gap in the samples. From a theoretical point of view, the gap is related to the chiral symmetry breaking and mass generation, a classical (unresolved) problem that has been explored at length in planar QED.[16,17] For the applications, it is by now clear that opening a gap in monolayer graphene will be a difficult task and efforts are concentrated on multilayer structures.[13,18,19]

In this paper, we analyze the stability of the Fermi points under small perturbations using very basic topological concepts.[20] We find that the Fermi points are protected by the discrete symmetries (translational invariance and space and time inversion) in the monolayer, bilayer AB, and multilayers with $ABCA\cdots$ (rhombohedral) stacking. The stability of Fermi points in stacks with the Bernal stacking $ABAB\cdots$ depends on the parity of the number of layers. We also discuss the changes in the low-energy and low-momentum properties induced by commensurate perturbations which hybridize the two K points and partially break translation invariance. We will not analyze here in detail the effects of spin-orbit coupling, which my lead to additional changes at low temperatures.[21–24]

The analysis reported here will be useful for the construction of continuum theories for long-wavelength spatial perturbations and for the study of the degeneracy and spectrum of the low index Landau levels in a magnetic field.

II. ELECTRONIC STRUCTURE AND STABILITY IN GRAPHENE

The Fermi surface (FS) is a central concept in condensed matter that controls the low-energy physics of the systems. In a Landau Fermi liquid at $T=0$, Luttinger[25] defined the FS of an interacting Fermi system in terms of the single-particle Green's function $G(\vec{k},\omega)$, as the solution of the equation $G^{-1}(\vec{k},0)=0$, and showed that it encloses the same volume, equal to the fermion density n, as in the noninteracting system. The robustness of the Fermi-liquid idea has been understood recently in the context of the renormalization group, where the Fermi and Luttinger liquids are seen as infrared fixed points.[26,27] In recent works,[28,29] Volovik has emphasized the idea of the topological stability of the Fermi surface as the origin of the robustness of the Fermi liquid and has suggested a classification of general fermionic systems in universality classes dictated by momentum space topology. A more recent proposal relates the stability of Fermi surfaces with K theory, a tool used to classify D-brane charges in string theory.[30] The idea behind the topological stability is to study the zeros of the matrix $G_0^{-1}(\vec{k},\omega)$ (free inverse propagator) that cannot be lifted by small perturbations. Here, we will analyze the stability of the Fermi points of single and multilayer graphenes, where the discrete symmetries of the system play a principal role. Although we will restrict ourselves to perturbations that can be studied within the context of a single-particle effective Hamiltonian, the extension to self-energy induced perturbations is rather straightforward and will be reported elsewhere.[31]

As shown in Fig. 1, monolayer graphene consists of a planar honeycomb lattice of carbon atoms. Corresponding to the two atoms in the unit cell, one may define two Bloch wave functions to be used in a variational (tight-binding) computation of the spectrum as follows:

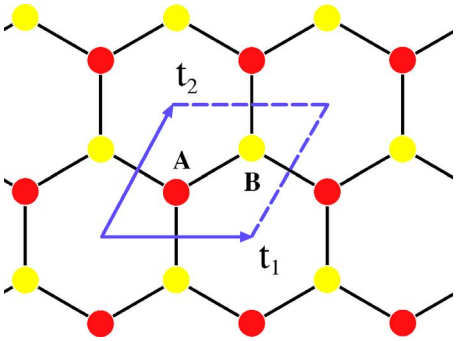

FIG. 1. (Color online) Direct lattice and unit cell for monolayer graphene.

$$\Phi_i(\vec{K}) = \sum_{\vec{t}} e^{i\vec{K}\cdot(\vec{r}_i+\vec{t})}\Phi(\vec{r}-\vec{r}_i-\vec{t}), \quad i=A,B, \tag{1}$$

where the sum runs over all the points in the direct lattice, i.e., $\vec{t}=n_1\vec{t}_1+n_2\vec{t}_2$, $(\vec{r}_A,\vec{r}_B)$ are the positions of the atoms in the unit cell, and $\Phi(\vec{r})$ is a real (π-type) atomic orbital. As is well known, a simple tight-binding computation[7,8] yields a spectrum with two Fermi points located at $\vec{K}_1=-2\vec{g}_1/3-\vec{g}_2/3$ and $\vec{K}_2=-\vec{K}_1$, where $\vec{t}_i\cdot\vec{g}_j=2\pi\delta_{ij}$ (see Fig. 2). Near the two Fermi points, the Hamiltonian can be linearized, and using appropriate units, one finds

$$H(\vec{K}_1+\vec{k}) \sim \begin{pmatrix} 0 & k^* \\ k & 0 \end{pmatrix} = k_x\sigma_x + k_y\sigma_y, \tag{2}$$

and $H(-\vec{K}_1+\vec{k})\sim -k_x\sigma_x+k_y\sigma_y$, where $k\equiv k_x+ik_y$ and σ_i are the Pauli matrices. Thus, the low-energy electronic excitations behave like massless Dirac fermions with relativistic spectrum $E=\pm|k|$.

Under a k-independent, translationally invariant perturbation,

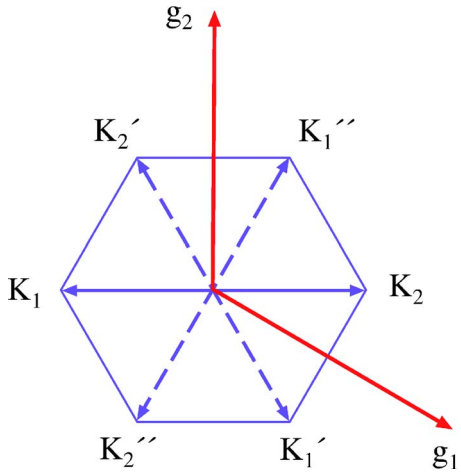

FIG. 2. (Color online) First Brillouin zone and Fermi points. The vectors $\vec{K}_1',\vec{K}_1''$ ($\vec{K}_2',\vec{K}_2''$) are equivalent to $\vec{K}_1$ ($\vec{K}_2$).

$$H(\vec{K}_1+\vec{k}) \to \begin{pmatrix} a_z & k^*+a^* \\ k+a & -a_z \end{pmatrix}, \tag{3}$$

where $a\equiv a_x+ia_y$, the spectrum becomes $E=\pm\sqrt{a_z^2+|k+a|^2}$ and a gap $2|a_z|$ is generated. This is consistent with Hořava's general arguments,[30] which show that Fermi points for Dirac fermions in two dimensions are unstable. However, this is not the end of the story, since the existence of discrete symmetries can sometimes stabilize the Fermi loci. In the case of the graphene, this role is played by time reversal $T:t\to -t$ and spatial inversion $I:(x,y)\to(-x,-y)$. The reality of the π orbitals implies that time reversal merely reverses $\vec{K}$,

$$T\Phi_i(\vec{K}) = \Phi_i^*(\vec{K}) = \Phi_i(-\vec{K}), \tag{4}$$

whereas the spatial inversion also exchanges the two types of atoms,

$$I\Phi_A(\vec{K}) = \Phi_B(-\vec{K}), \quad I\Phi_B(\vec{K}) = \Phi_A(-\vec{K}). \tag{5}$$

Invariance under these symmetries imposes the following constraints on the Hamiltonian:

$$T{:}H(\vec{K}) = H^*(-\vec{K}),$$

$$I{:}H(\vec{K}) = \sigma_x H(-\vec{K})\sigma_x. \tag{6}$$

Although these are useful properties that relate the Hamiltonians at opposite values of $\vec{K}$, what we need is a constraint on the form of $H(\vec{K})$. This is obtained by combining time reversal with the spatial inversion,

$$TI{:}H(\vec{K}) = \sigma_x H^*(\vec{K})\sigma_x, \tag{7}$$

implying $H_{11}(\vec{K})=H_{22}(\vec{K})$. This enforces $a_z=0$ in Eq. (3), and we see that no gap opens if the perturbation preserves the space-time inversion TI.

This has an interesting topological interpretation, which extends the previous arguments to k-dependent—but translationally invariant—perturbations. The low-energy Hamiltonian $H(\vec{K}_1+\vec{k})$ in Eq. (2) defines a map from the circle $k_x^2+k_y^2=R^2$ to the space of 2×2 Hamiltonians $H=\vec{h}\cdot\vec{\sigma}$:

$$k = Re^{i\theta} \to (h_x,h_y,h_z) = R(\cos\theta,\sin\theta,0). \tag{8}$$

Since Fermi points correspond to zeros of the determinant $-\det(H)=h_x^2+h_y^2+h_z^2$, a perturbation will be able to create a gap only if the loop represented by the map (8) is contractible in the space Hamiltonians with nonvanishing determinants, which are just $R^3-\{0\}$. This is clearly the case, since $\pi_1(R^3-\{0\})=\pi_1(S^2)=0$. On the other hand, Hamiltonians invariant under TI are represented by points in R^2, and we have

$$\pi_1(R^2-\{0\}) = \pi_1(S^1) = Z. \tag{9}$$

This means that nontrivial maps such as the ones implied by Eq. (2) can only be extended to the interior of the circle by going through the origin, i.e., by having at least one zero. This precludes the creation of a gap.

Note that the maps defined by the low-energy Hamiltonian in the proximity of the two Fermi points,

$$H(\pm\vec{K}_1+\vec{k}):k=Re^{i\theta}\rightarrow h_x+ih_y=\pm Re^{\pm i\theta}, \tag{10}$$

have opposite winding numbers $N=\pm 1$, which can be computed by the formula

$$N=\frac{1}{4\pi i}\int_0^{2\pi} d\theta\,\mathrm{Tr}(\sigma_z H^{-1}\partial_\theta H). \tag{11}$$

The fact that the two Dirac points carry opposite charges suggests that they could annihilate mutually if brought together by a perturbation. Any external potential commensurate with the honeycomb lattice, which has a finite Fourier component at the wave vector $\vec{G}=\vec{K}_1-\vec{K}_2$, induces terms which hybridize the two Dirac points, and it will lead to the possibility of a gap. We can compute all the possible perturbations which are compatible with the symmetries of the lattice. The most general (4×4) Hamiltonian including perturbations at $\vec{G}=0$ and $\vec{G}=\vec{K}_1-\vec{K}_2\equiv-\vec{K}_1$ is

$$\mathcal{H}\equiv\begin{pmatrix} 0 & k^*+Q_1^* & Q_2 & Q_4 \\ k+Q_1 & 0 & Q_4 & Q_3 \\ Q_2^* & Q_4^* & 0 & -k+Q_1 \\ Q_4^* & Q_3^* & -k^*+Q_1^* & 0 \end{pmatrix}, \tag{12}$$

where $Q_1=Q_1^x+iQ_1^y$ transforms according to the E_2 representation of the C_{6v} symmetry group[32] at the $\Gamma(\vec{K}=0)$ point. Q_2 and Q_3 belong to the E representation of the C_{3v} group at $\vec{K}_1$, and Q_4 to the A_1 representation of the same group (see Ref. 33 for notation). At this point, it is worth noticing a point on notation. When grouping the Hamiltonians attached to the two Dirac points $(K_{1,2})$ into a four-dimensional matrix, it is a common practice to reverse the order of the sublattices (A,B) in one of the Fermi points in such a way that the four-dimensional wave functions have the form

$$\psi=(\Phi_{K_1,A},\Phi_{K_1,B},\Phi_{K_2,B},\Phi_{K_2,A}).$$

If this is done, the topological structure of the Hamiltonian is messed up and the computation of charges becomes less clear. For this reason, we follow instead the convention in Ref. 21, where

$$\psi=(\Phi_{K_1,A},\Phi_{K_1,B},\Phi_{K_2,A},\Phi_{K_2,B}).$$

This is also important if one tries to compare the analysis of the perturbations written in Eq. (12) with the ones produced by the different types of disorder.[34–36]

The perturbation given by Q_1^x and Q_1^y shifts the Dirac points but does not open a gap. In fact, the only parameter which opens a gap is Q_4. When only Q_4 is different from zero, the spectrum becomes $E=\pm\sqrt{|Q_4|^2+|k|^2}$ and, for Q_4 real, the deformation of the lattice is given in Fig. 3, where one can see that no point symmetry is broken. This shows, in particular, that invariance under space-time inversion is *not* enough to guarantee the stability of Fermi points—translation invariance plays a crucial role: *TI* by itself makes the Fermi points *individually* stable, but they may still annihilate each other in the presence of a perturbation that breaks translation invariance. A distortion of the type of Q_4 can be induced by a substrate with a periodicity commensurate with the lattice, or by the effect of one layer on another when there is a lattice mismatch between them, as in samples grown on a substrate.[3,37] It can be responsible for the gap observed recently in photoemission experiments.[38] It is worth noting that the perturbation denoted here Q_4 has been studied in a graphene ribbon in Ref. 39.

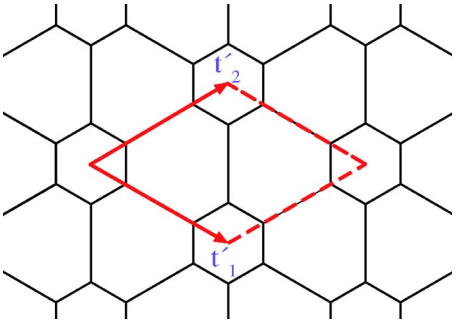

FIG. 3. (Color online) Distortion caused by the condensation of A_1 mode with real Q_4 and new unit cell.

When only Q_2 or Q_3 is different from zero, we find

$$\epsilon_k=\pm\frac{|Q_{2,3}|}{2}\pm\sqrt{\frac{|Q_{2,3}|^2}{4}+|\vec{k}|^2}. \tag{13}$$

The energy bands are represented in Fig. 4 for the particular case $Q_2=0$, $Q_3=1$. We can see that the spectrum is the same as the one obtained in a simple model for a bilayer system,[40] which will be discussed later. A complete analysis of the most general perturbation of the form (12) will be given elsewhere.[31]

In the absence of time-reversal symmetry, other perturbations are possible, such as

$$\delta\mathcal{H}=B_1\sigma_z\tau_z+B_2\sigma_y\tau_y, \tag{14}$$

where σ and τ are Pauli matrices whose entries are the sublattice and K point indices, respectively, and B_1 and B_2 transform like the z component of a magnetic field and are odd under time inversion. Note that the first term is the orbital part of the intrinsic spin-orbit coupling in graphene,[21–24] and it opens a gap. The second term should appear in a general spin-orbit Hamiltonian which takes into account the coupling between the two K points.

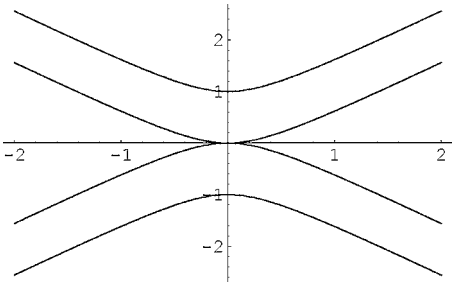

FIG. 4. Energy bands along the line $(0,k_y)$ for $Q_3=1$, $Q_4=0$.

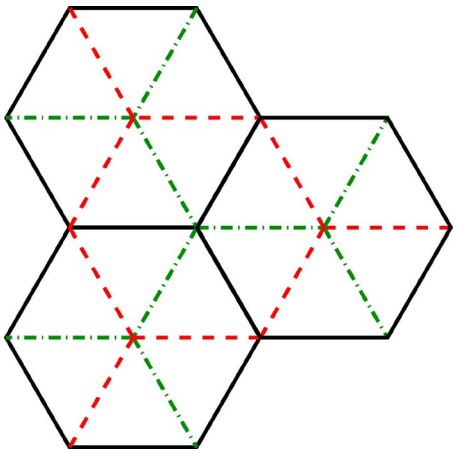

FIG. 5. (Color online) Sketch of the three possible positions of a given layer with respect to the others in a graphene stack. Bernal stacking, 1,2,1,2,…, is described by two inequivalent planes, while orthorhombic stacking, 1,2,3,1,2,3,…, requires the three inequivalent ones.

III. ELECTRONIC STRUCTURE AND STABILITY IN MULTILAYERED GRAPHENE

The case of the multilayer is more interesting. We will concentrate on the ability of the *TI* invariance to prevent the creation of a gap. For the sake of definiteness, only staggered (*ABA*) and rhombohedral (*ABC*) stackings will be considered. The relative orientations of the *ABC* planes are sketched in Fig. 5. The two inequivalent atoms in layer n will be denoted (A_n, B_n). Our conventions are such that the couplings of an A_n (B_n) atom to the three in-plane nearest neighbors are shaped as a Y (inverted Y), independent of n. Thus, the low-energy limit of the "free" Hamiltonian obtained by neglecting interlayer couplings is block diagonal, with 2×2 blocks given by Eq. (2)

The simplest model introduces interlayer hoppings t only between nearest neighbors. The resulting Hamiltonian for bilayer graphene in the vicinity of the K_1 Fermi point is

$$\mathcal{H}(k) = \begin{pmatrix} 0 & k^* & 0 & t \\ k & 0 & 0 & 0 \\ 0 & 0 & 0 & k^* \\ t & 0 & k & 0 \end{pmatrix}, \tag{15}$$

and the energy bands are given by Eq. (13) with the replacement $|Q_{2,3}| \to t$. In the limit $E \ll t$, one can obtain an effective Hamiltonian[40] for the lowest-energy bands. To this end, reorder the wave functions according to $(A_1, B_1, A_2, B_2) \to (A_2, B_1, A_1, B_2)$, so that in the new basis the Hamiltonian becomes

$$\mathcal{H}(k) = \begin{pmatrix} 0 & 0 & 0 & k^* \\ 0 & 0 & k & 0 \\ 0 & k^* & 0 & t \\ k & 0 & t & 0 \end{pmatrix} \equiv \begin{pmatrix} H_{11} & H_{12} \\ H_{21} & H_{22} \end{pmatrix}, \tag{16}$$

where H_{ij} is a 2×2 block. The identity

$$\det(\mathcal{H} - E) = \det(H_{11} - H_{12}(H_{22} - E)^{-1}H_{21} - E)\det(H_{22} - E) \tag{17}$$

shows that, for $E \ll t$, the substitution $H_{22} - E \to H_{22}$ reduces the computation of the lowest-energy bands to the diagonalization of the 2×2 effective Hamiltonian,

$$\mathcal{H}^{eff} \equiv H_{11} - H_{12}H_{22}^{-1}H_{21} = -\frac{1}{t}\begin{pmatrix} 0 & k^{*2} \\ k^2 & 0 \end{pmatrix}. \tag{18}$$

This effective Hamiltonian involves only the atoms (A_2, B_1), which are not linked by t and give rise to bands with zero energy at the Fermi points. Since (A_2, B_1) are interchanged under spatial inversion $\vec{r} \to -\vec{r}$, the combined *TI* invariance imposes a constraint $\mathcal{H}^{eff}(k) = \sigma_x \mathcal{H}^{eff*}(k)\sigma_x$ identical to Eq. (7). This implies $\mathcal{H}_{11}^{eff}(k) = \mathcal{H}_{22}^{eff}(k)$, which shows that no gap can open. According to Eq. (11), the topological charge for the $\vec{K}_1$ Fermi point is +2 and, by time-reversal invariance, the charge for $-\vec{K}_1$ is −2. Thus, as in the case of monolayer graphene, the Fermi points are stable under perturbations that preserve *TI* and translation invariance. For instance, a perturbation such as trigonal warping[40] changes the off-diagonal elements in Eq. (18), $k^2 \to k^2 + v_3 k^*$, and splits the Fermi point of charge $Q = +2$ into three Dirac points away from the K point, and charge $Q = +1$, and another Dirac point at the K point and $Q = -1$, but the total charge is conserved and no gap opens. However, a perturbation hybridizing $\vec{K}_1$ and $-\vec{K}_1$ or one breaking *TI* might lead to a gapped system with no Fermi points at all. A physical example is provided by the experiment described in Ref. 18, where a gap is controlled by changing the carrier concentration in each layer.

This analysis can be easily generalized to multilayer graphene with rhombohedral stacking. This type of staking includes the links $(B_1 - A_2, B_2 - A_3, \ldots, B_{N-1} - A_N)$, and the effective Hamiltonian, which involves only the unlinked atoms (A_1, B_N), is given by

$$\mathcal{H}^{eff} = -\frac{1}{t^{N-1}}\begin{pmatrix} 0 & k^{*N} \\ k^N & 0 \end{pmatrix}. \tag{19}$$

The topological charge for the $\vec{K}_1$ ($-\vec{K}_1$) Fermi point is $+N$ ($-N$). As the point group for multilayer graphene with rhombohedral stacking is D_{3d}, which contains the inversion I, the system is invariant under *TI*, which interchanges (A_1, B_N), and the whole argument goes through as before. Thus, we conclude that the Fermi points for multilayer graphene with rhombohedral stacking are stable against perturbations that respect *TI* and translation invariance.

The situation is very different for *ABA* stacking. An N-layer graphene stack is invariant under the spatial inversion I only for even N, where the point group is D_{3d}, while it is D_{3h} for odd N.

The $2N$ eigenstates in a stack with N layers at $k = 0$ can be divided into two sets: N states at the orbitals connected by the interlayer hopping t and N states in the other sublattice sites of each layer. If we only consider the hopping t, the first N states acquire a dispersion[41] lying in the range $-2t \leqslant \epsilon \leqslant 2t$. The other N states are degenerate with $\epsilon = 0$. A perturbation compatible with all the symmetries of the stack is a

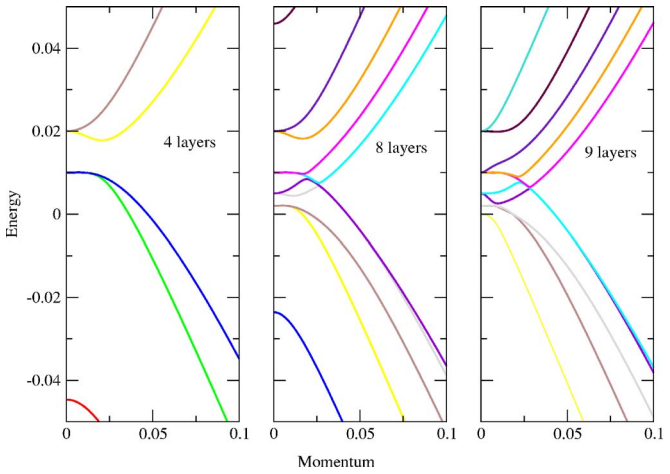

FIG. 6. (Color online) Energy bands close to $\epsilon=0$ for a stack with four layers (left), eight layers (center), and nine layers (right). All stacks have the Bernal stacking. The Fermi velocity is $v_F=1$, $t=0.1$, and a layer dependent shift has been included: $\epsilon_n \equiv \{0.02, 0.01\}$ (left), $\epsilon_n \equiv \{0.02, 0.01, 0.005, 0.002\}$ (center), and $\epsilon_n \equiv \{0.02, 0.01, 0.005, 0.002, 0\}$ (right).

layer dependent shift of the on-site energies. This shift can be arbitrary, except for the twofold degeneracy related to the equivalence between layers which are symmetrically placed around the center, $\epsilon_n=\epsilon_{N-n+1}$. This is illustrated in Fig. 6.

The results in Fig. 6 show a gap at half filling in the stack with four layers, and overlapping bands at all energies for the stack with eight and nine layers. Note that the gap in the stack with four layers does not require the existence of an external electric field, which will break the equivalence of the layers at opposite sides of the stack. In all stacks with an even number of layers, the two bands which start at the on-site energy of layers n and $N-n+1$ are degenerate at $k=0$. The effective 2×2 Hamiltonian describing the bands near these degeneracy points has off-diagonal elements with a nontrivial phase as in Eq. (18). Hence, the degeneracy has topological charge $Q=2$, and it cannot be removed by perturbations compatible with the symmetries of the stack. For even n, an explicit computation shows that these two bands will have curvatures with the same sign near $k=0$. Thus, the corresponding degeneracy points do not represent Fermi points. For odd numbered layers, the two bands disperse in opposite directions away from $k=0$, and the degeneracy points become stable Fermi points at the appropriate doping. Note that the symmetries of the system allow for a direct trigonal-like coupling between the two layers, which will split this Fermi point and give rise to four Fermi points showing linear dispersion, as in the bilayer. On physical grounds, this coupling will be negligible, unless the two layers are contiguous.

The low-energy bands in a stack with an odd number of layers also contain doubly degenerate states at $k=0$, associated with the equivalence between layers at opposite sides of the stack. In this case, the inversion I is not part of the symmetry group D_{3h} of the stack, no invariance under TI can be imposed, and, as a consequence, the first homotopy group π_1 is trivial. This means that no conserved topological charge exists. Hence, a gap may open at $k=0$ when other perturbations consistent with the symmetries of the stack are included. Concretely, a direct coupling between orbitals in the same sublattice in layers separated by an odd number of other layers will open a gap. Such a coupling, between layers which are second nearest neighbors, has been proposed in graphite.[42]

IV. CONCLUSIONS

We have presented a classification of the bands at low momenta and low energy of graphene layers and stacks with many layers.

Each Fermi point in single layer graphene is stable against perturbations which preserve the discrete TI symmetry and which do not mix the two Fermi points. A magnetic field, for instance, induces a gap in the spectrum, see Eq. (14). This term arises from the discreteness of the lattice, and it should be of higher order than the minimal coupling which leads to the formation of Landau levels. Combining this and dimensional arguments, we expect it to be $B_1 \propto (v_F/l_B)\times(a/l_B)$, where a is the lattice constant and $l_B=\sqrt{(eB)/(c\Phi_0)}$ is the cyclotron radius. Thus, for $B\sim 10$ T, we have $B_1 \approx 0.1$ meV.

We have also classified the long-wavelength perturbations commensurate with the graphene lattice, which can hybridize the two K points. Some of these perturbations open a gap in the spectrum, while others shift the position of the Dirac points. We expect that their strength will decay like a power law with the wavelength of the distortion.

The low-energy and low-momentum spectrum of stacks with many graphene layers depends on the stacking order and the number of layers. For the most common case of the Bernal stacking, we find that layer dependent on-site energies lead to Fermi points with double degeneracy, topological charge $Q=\pm 2$, and a parabolic dispersion in k. This situation will be stable in stacks with a large (even) number of layers. In stacks with an odd number of layers, there is no conserved topological charge and this degeneracy will be broken by additional interactions. Stacks with rhombohedral order lead to degenerate states with a large topological charge, $Q=N$, which will give rise to the formation of a cascade of Fermi points slightly away from $k=0$, with lower topological charges.

The most likely origin of the inequivalence between layers is the charge accumulation at the layers close to the surface.[43] An induced doping of $10^{10}-10^{12}$ cm^{-2} gives rise to shifts in the local potential of 0.01–0.1 eV, so that the splittings associated with this effect can be easily measurable. We find that a true gap opens, in the absence of an external field which breaks spatial inversion, only in a stack with four layers and Bernal stacking. Finally, stacking defects, which break the equivalence between pairs of layers, will also break the degeneracy of all bands at $k=0$.

ACKNOWLEDGMENTS

It is a pleasure to thank J. J. Manjarín and M. A. Valle-

Basagoiti for useful discussions. M.A.H.V. and F.G. are thankful to the MEC (Spain) for financial support through Grant No. FIS2005-05478-C02-01 and the European Union Contract No. 12881 (NEST). J.L.M. has been supported in part by the Spanish Science Ministry under Grant No. FPA2005-04823. One of us (F.G.) also acknowledges support from the Comunidad de Madrid, through the program CIT-ECNOMIK, CM2006-S-0505-ESP-0337.

[1] K. S. Novoselov, A. K. Geim, S. V. Morozov, D. Jiang, Y. Zhang, S. V. Dubonos, I. V. Gregorieva, and A. A. Firsov, Science **306**, 666 (2004).
[2] K. S. Novoselov, D. Jiang, T. Booth, V. Khotkevich, S. M. Morozov, and A. K. Geim, Proc. Natl. Acad. Sci. U.S.A. **102**, 10451 (2005).
[3] C. Berger, Z. Song, T. Li, X. Li, A. Y. Ogbazghi, R. Feng, Z. Dai, A. N. Marchenkov, E. H. Conrad, and P. N. First, J. Phys. Chem. B **108**, 19912 (2004).
[4] K. S. Novoselov, A. K. Geim, S. V. Morozov, D. Jiang, M. I. Katsnelson, I. V. Grigorieva, S. V. Dubonos, and A. A. Firsov, Nature (London) **438**, 197 (2005).
[5] Y. Zhang, Y.-W. Tan, H. L. Stormer, and P. Kim, Nature (London) **438**, 201 (2005).
[6] Y. Kopelevich, J. H. S. Torres, R. R. da Silva, F. Mrowka, H. Kempa, and P. Esquinazi, Phys. Rev. Lett. **90**, 156402 (2003).
[7] P. R. Wallace, Phys. Rev. **71**, 622 (1947).
[8] J. C. Slonczewski and P. R. Weiss, Phys. Rev. **109**, 272 (1958).
[9] J. González, F. Guinea, and M. A. H. Vozmediano, Phys. Rev. Lett. **69**, 172 (1992).
[10] J. González, F. Guinea, and M. A. H. Vozmediano, Nucl. Phys. B **406**, 771 (1993).
[11] S. Zhou, G.-H. Gweon, J. Graf, A. Fedorov, C. Spataru, R. Diehl, Y. Kopelevich, D.-H. Lee, S. G. Louie, and A. Lanzara, cond-mat/0608069, Nat. Phys. (to be published).
[12] J. Nilsson, A. H. Castro Neto, N. M. R. Peres, and F. Guinea, Phys. Rev. B **73**, 214418 (2006).
[13] J. Nilsson, A. H. Castro Neto, F. Guinea, and N. M. R. Peres, Phys. Rev. Lett. **97**, 266801 (2006).
[14] K. S. Novoselov, E. McCann, S. V. Morozov, V. I. Falko, M. I. Katsnelson, U. Zeitler, D. Jiang, F. Schedin, and A. K. Geim, Nat. Phys. **2**, 177 (2006).
[15] S. Zhou, G.-H. Gweon, and A. Lanzara, Ann. Phys. (N.Y.) **321**, 1730 (2006).
[16] T. Appelquist, D. Nash, and L. C. R. Wijewardhana, Phys. Rev. Lett. **60**, 2575 (1988).
[17] D. V. Khveshchenko, Phys. Rev. Lett. **87**, 246802 (2001).
[18] T. Ohta, A. Bostwick, T. Seyller, K. Horn, and E. Rotenberg, Science **313**, 951 (2006).
[19] E. V. Castro, K. S. Novoselov, S. V. Morozov, N. M. R. Peres, J. L. dos Santos, J. Nilsson, F. Guinea, A. K. Geim, and A. H. C. Neto, cond-mat/0611342 (unpublished).
[20] M. Nakahara, *Geometry, Topology and Physics* (IOP, Bristol, 2003).
[21] C. L. Kane and E. J. Mele, Phys. Rev. Lett. **95**, 226801 (2005).
[22] D. Huertas-Hernando, F. Guinea, and A. Brataas, Phys. Rev. B **74**, 155426 (2006).
[23] H. Min, J. E. Hill, N. A. Sinitsyn, B. R. Sahu, L. Kleinman, and A. H. MacDonald, Phys. Rev. B **74**, 165310 (2006). cond-mat/0606504.
[24] Y. Yao, F. Ye, X.-L. Qi, S.-C. Zhang, and Z. Fang, Phys. Rev. B **75**, 041401(R) (2007).
[25] J. Luttinger, Phys. Rev. **119**, 1153 (1960).
[26] J. Polchinski, in *Proceedings of the 1992 Theoretical Advanced Institute in Elementary Particle Physics*, edited by J. Harvey, and J. Polchinski (World Scientific, Singapore, 1993).
[27] R. Shankar, Rev. Mod. Phys. **66**, 129 (1994).
[28] G. E. Volovik, *The Universe in a Helium Droplet* (Clarendon, Oxford, 2003).
[29] G. E. Volovik, cond-mat/0601372 (unpublished).
[30] P. Hořava, Phys. Rev. Lett. **95**, 016405 (2005).
[31] J. Mañes, P. Guinea, and M. A. H. Vozmediano (unpublished).
[32] The actual symmetry group of monolayer graphene is D_{6h}, but, as long as we restrict ourselves to in-plane distortions of the lattice, it is sufficient to consider the subgroup C_{6v}. That is what we do in this paper, since out-of-plane distortions (phonons) cannot couple linearly to electrons.
[33] C. J. Bradley and A. P. Cracknell, *The Mathematical Theory of Symmetry in Solids* (Clarendon, Oxford, 1972).
[34] A. Altland, cond-mat/0607247 (unpublished).
[35] E. McCann, K. Kechedzhi, V. I. Falko, H. Suzuura, T. Ando, and B. L. Altshuler, Phys. Rev. Lett. **97**, 146805 (2006).
[36] I. L. Aleiner and K. B. Efetov, Phys. Rev. B **74**, 075102 (2006).
[37] C. Berger, Z. Song, X. Li, X. Wu, N. Brown, C. Naud, D. Mayou, T. Li, J. Hass, A. N. Marchenkov, E. H. Conrad, P. N. First, and W. A. de Heer, Science **312**, 1191 (2006).
[38] A. Lanzara (private communication).
[39] D. Gunlycke, H. Lawler, and C. T. White, Phys. Rev. B **75**, 085418 (2007).
[40] E. McCann and V. I. Fal'ko, Phys. Rev. Lett. **96**, 086805 (2006).
[41] F. Guinea, A. H. Castro Neto, and N. M. R. Peres, Phys. Rev. B **73**, 245426 (2006).
[42] R. O. Dillon, I. L. Spain, and J. W. McClure, J. Phys. Chem. Solids **38**, 635 (1977).
[43] F. Guinea, cond-mat/0611185 (unpublished).